Exploring Kitaev Physics in Honeycomb Magnets $A_3Ni_2XO_6$ (A = Li, Na; X = Bi, Sb): Insights from First-Principles Calculations

Shi-Bo Zhao(赵世博), Jia-WanLi(李家万), and Yusheng Hou(侯玉升)*

Guangdong Provincial Key Laboratory of Magnetoelectric Physics and Devices, Center for Neutron Science and Technology, School of Physics, Sun Yat-Sen University, Guangzhou 510275, China

(Received 24 May 2025; accepted manuscript online 5 September 2025)

Magnets exhibiting the Kitaev interaction, a bond-dependent magnetic interaction in honeycomb lattices, are generally regarded as promising candidates for hosting novel phenomena like quantum spin liquid states. However, realizing such magnets remains a significant challenge. Recently, some studies have suggested honeycomb magnets $A_3Ni_2XO_6$ (A = Li, Na; X = Bi, Sb) with a high spin $S = 1$ could serve as potential candidates for realizing strong Kitaev interactions. In this work, we systematically investigate their magnetic properties, with a particular emphasis on their Kitaev interactions, using first-principles calculations and Monte Carlo simulations. Our results indicate that all $A_3Ni_2XO_6$ compounds are zigzag antiferromagnets, and their magnetic moments almost tend to be out of plane. We find that their dominant magnetic interactions are the nearest-neighbor ferromagnetic and third-nearest-neighbor antiferromagnetic Heisenberg interactions, while their Kitaev interactions are extremely weak. By analyzing their electronic structures and the mechanism of generating their magnetic interactions, we reveal that either artificially tuning spin–orbit coupling or applying strain cannot produce sufficient spin–orbit entangled states to realize the intriguing Kitaev interactions. Our work advances the understanding of the magnetism in $A_3Ni_2XO_6$ compounds and provides insights for further exploration of Kitaev physics in honeycomb magnets.

DOI: 10.1088/0256-307X/42/10/100708 CSTR: 32039.14.0256-307X.42.10.100708

1. Introduction. Quantum spin liquids (QSLs) exhibit the potential to enable a new form of topologically protected quantum computation and novel physical phenomena, including fractional excitations.[1,2] Kitaev proposed a creative model for bond-dependent interactions of spin 1/2 on the two-dimensional (2D) honeycomb lattice, which provides a rare example of well-established QSLs.[3] In recent years, the Kitaev model has sparked extensive research interest due to its exactly solvable ground state and rich physics.[4,5] In particular, it has been demonstrated that spin–orbit entangled Mott insulators are expected to realize Kitaev interactions.[6] Such Mott insulators tend to be transition metal oxides with partially filled 4d and 5d shells, as their local magnetic moments originate from spin–orbit entangled $J_{\rm eff} = 1/2$ Kramers doublets.[6] For instance, honeycomb magnets iridium oxides A_2IrO_3 (A = Na or Li)[7] and α-$RuCl_3$[8] are widely regarded as candidates for realizing Kitaev QSL. Nevertheless, the definite evidence of the existence of Kitaev QSL in A_2IrO_3 and α-$RuCl_3$ remains elusive so far. In fact, they exhibit the long-range zigzag antiferromagnetic (AFM) order at very low temperatures.[9–11] Theoretically, it is demonstrated that the appearance of long-range zigzag AFM orders in them is attributed to other non-Kitaev interactions such as the Heisenberg exchange interaction and bond-dependent off-diagonal exchange.[10,12–14]

Since its ground state is also described by a spin–orbit entangled Kramers doublet, the pseudospin-1/2 state of a high-spin $3d^7$ electron configuration under an octahedral crystal field and strong spin–orbit coupling (SOC) has been proposed to realize Kitaev interactions.[15,16] Such a $3d^7$ electron configuration corresponds to a $t_{2g}^5e_g^2$ arrangement with $S = 3/2$ and effective $L = 1$. Due to the presence of spin-active e_g electrons, the ferromagnetic (FM) Kitaev coupling predominates over other non-Kitaev couplings.[15] Furthermore, 3d orbitals are more localized than 4d and 5d orbitals, which theoretically reduces the unwanted long-range interactions and non-Kitaev terms. Guided by this mechanism, honeycomb magnets containing high-spin $3d^7$ magnetic ions Co^{2+}, such as $Na_3Co_2SbO_6$ and $Na_2Co_2TeO_6$,[15] are theoretically considered the most promising candidates for realizing the Kitaev spin liquid phase. Of particular interest is $Na_3Co_2SbO_6$, which can be driven into the Kitaev spin liquid phase by applying strain or pressure.[17] Although some experimental studies have provided positive evidence supporting the theoretically predicted Kitaev physics in high-spin $3d^7$ magnets, conclusive verification remains elusive so far.[18–23] Even worse, some investigations have suspected the validity of Kitaev physics in Co-based honeycomb magnets.[24,25] Therefore, whether Kitaev interactions exist in Co-based honeycomb magnets is still a topic of ongoing debate, and it is necessary to expand new paths toward searching for new candidates of Kitaev spin liquids.

*Corresponding author. Email: houysh@mail.sysu.edu.cn

© 2025 Chinese Physical Society and IOP Publishing Ltd. All rights, including for text and data mining, AI training, and similar technologies, are reserved.

In recent years, the theoretical research on Kitaev physics has been extended to higher-spin systems, such as $S = 1$ and $3/2$.[26,27] According to these studies, non-negligible Kitaev interactions, induced by the strong SOC from heavy ligands, may occur in some transition metal compounds such as $CrSiTe_3$,[27] CrI_3, $CrGeTe_3$,[28–30] NiI_2,[31,32] and $1T$-$CrTe_2$.[33] In addition, another group of potential candidates comprises the layered transition metal oxide compounds $A_3Ni_2XO_6$ (A = Li, Na; X = Bi, Sb).[26] Similar to the aforementioned high-spin $3d^7$ Kitaev magnets, strong SOC may arise due to proximity to the heavy X atoms, presenting a new pathway to the realization of Kitaev interactions.[26] Notably, the specific heat measurements of both $Li_3Ni_2SbO_6$ (LNSO) and $Na_3Ni_2SbO_6$ (NNSO) reveal an entropy of approximately $\frac{1}{2}\log 3$ per Ni above their Néel temperatures. This strongly suggests that they are promising candidates for Kitaev honeycomb magnets with $S = 1$.[34] Moreover, a recent experiment observed that $Na_3Ni_2BiO_6$ (NNBO) exhibits a $\frac{1}{3}$ magnetization plateau under an applied magnetic field and suggested the strong influence of non-negligible Kitaev interactions on this exotic plateau.[35] However, these results are not sufficient to conclude that Kitaev interactions exist in $S = 1$ honeycomb magnets $A_3Ni_2XO_6$. Therefore, current research on the magnetic interactions of NNBO, particularly those involving Kitaev interactions, remains highly valuable and intriguing.

In this work, we systematically investigate the magnetic properties of $A_3Ni_2XO_6$ using first-principles calculations and Monte Carlo simulations. We first examine their magnetic ground states and confirm that they are indeed antiferromagnets with zigzag order. Additionally, our calculations reveal that most of these compounds possess an out-of-plane magnetic easy axis. These fundamental magnetic properties are largely consistent with previous experimental and theoretical studies.[34,36,37] Employing a modified four-state method and a small angle method,[14,38] we identify that the dominant magnetic interactions include the nearest-neighbor (NN) FM Heisenberg, long-range third-NN AFM Heisenberg, and biquadratic interactions. Surprisingly, the desired Kitaev interactions are rather weak compared to the dominating Heisenberg interactions. By artificially enlarging the magnitude of the SOC of Bi or Ni atoms, we demonstrate that Kitaev interactions are not enhanced and the nature of the dominant Heisenberg interactions is also not affected. Through an analysis of the electronic structures and the mechanism of generating the magnetic interactions, we reveal that artificially controlling SOC and applying strain cannot induce dominant orbital moments favorable for Kitaev interactions. Based on these results, we deem that Kitaev interactions are very weak in $A_3Ni_2XO_6$. The present work contributes to the understanding and exploration of Kitaev physics in $A_3Ni_2XO_6$ and offers insights for promoting the realization of Kitaev spin liquids in these compounds.

2. Computational Details and Methods. Our first-principles calculations based on the density functional theory (DFT) are performed with the Vienna *ab initio* simulation package (VASP) at the level of the generalized gradient approximation.[39–42] We employ the projector-augmented-wave pseudopotentials to describe core-valence interactions.[43] We treat Ni 3d4s, O 2s2p, Na 2p3s, Li 1s2s, Bi 5d6s6p and Sb 5s5p as valence electrons in our calculations. The energy cutoff of plane-wave expansions is set to 400 eV for $Na_3Ni_2XO_6$ but 500 eV for $Li_3Ni_2XO_6$, reflecting differences in the pseudopotentials of Na and Li. The energy convergence criterion is set to 10^{-6} eV in self-consistent calculations. To account for the electron correlation associated with the Ni 3d electron, we adopt the simplified rotationally invariant DFT+U method proposed by Dudarev.[44] The effective electron correlation parameter $U_{\text{eff}} = U - J = 4.5$ eV with $U = 5.5$ eV and $J = 1.0$ eV[34] is adopted in our work.

In our calculations, we adopt the experimentally measured monoclinic crystal structures with the space group $C2/m$.[36,45–47] The bilinear magnetic interaction parameters considering the SOC are calculated using a variant of the previously developed four-state method.[14,48] We employ the $3\times3\times1$ supercells of $A_3Ni_2XO_6$ and $3\times3\times7$ Γ-centered k-point grids to calculate magnetic interaction parameters. Since the bond-dependent Kitaev interactions align along the Ni-O bonds of the NiO_6 octahedra, we rotate the global coordinate system to the local one as illustrated by the yellow dashed lines in Fig. 1(a). For the strain simulations, we apply a 5% lattice constant strain to the lattice structure in all three spatial directions. Positions of all atoms are fully relaxed until the magnitude of force on each atom is less than 0.01 eV/Å, and a $9\times5\times9$ Γ-centered k-point grid is employed in these computations. Notably, the relaxed crystal structure under strain retains its space group $C2/m$.

3. Results and Discussion. We first discuss the crystal structure of $A_3Ni_2XO_6$. As shown in Figs. 1(a) and 1(b), $A_3Ni_2XO_6$ exhibits a quasi-2D structure with space group $C2/m$, where the $S = 1$ Ni^{2+} ions form a honeycomb lattice in the ab plane. The structure consists of ordered mixed layers containing magnetic Ni^{2+} cations and non-magnetic X^{5+} cations, which alternate with alkali metal layers. Each Ni atom is coordinated by six oxygen atoms, forming a NiO_6 octahedron. These octahedra are connected via edge-sharing to form a network in the ab plane [see the gray octahedra in Fig. 1(a)]. Table S1 of the Supplementary Materials (SM) lists the lattice constants of $A_3Ni_2XO_6$. Notably, NNBO exhibits the largest lattice constant, while LNSO exhibits the smallest, consistent with the ionic radii of their constituent atoms.

Honeycomb magnets typically exhibit complex magnetic ground states as a result of their intricate and/or frustrated magnetic interactions. Due to the competition among the first three NN magnetic interactions in honeycomb magnets,[49,50] four typical magnetic orders can be stabilized, including the FM, Néel AFM, stripe AFM, and zigzag AFM orders [Figs. 1(c)–1(f)]. To have a first glance at the magnetic ground states of $A_3Ni_2XO_6$, we calculate the total energies of these four magnetic orders

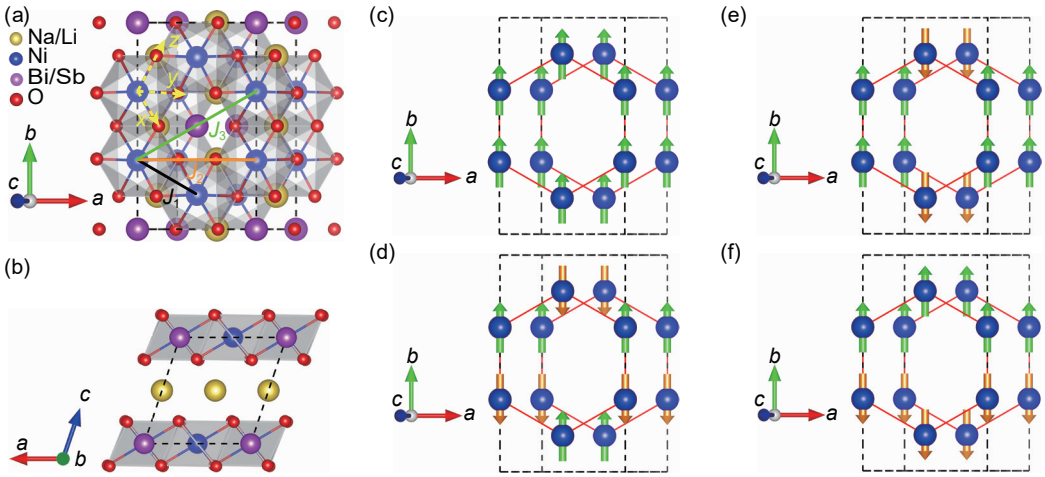

Fig. 1. (a) Top view and (b) side view of the crystal structures of $A_3Ni_2XO_6$ (A = Li, Na; X = Bi, Sb), where black dashed lines represent the unit cell of $A_3Ni_2XO_6$, the gray polyhedra represent the NiO_6 octahedra, the black, orange and green solid lines indicate NN, second-NN, and third-NN magnetic interactions. (c) FM order. (d) Néel AFM order. (e) Stripe AFM order. (f) Zigzag AFM order. In (c)–(f), the up and down spins of magnetic Ni^{2+} ions are shown by the green and brown arrows, respectively.

without considering SOC. Our calculations indicate that all $A_3Ni_2XO_6$ compounds exhibit the zigzag AFM magnetic ground state (Fig. S1 in the SM). To further confirm the magnetic ground states, we estimate their magnetic interaction parameters through the energy-mapping method.[51] Based on previous theoretical work[50] and neglecting SOC, we adopt the following spin exchange Hamiltonian:

$$H = J_1 \sum_{\langle ij \rangle} S_i \cdot S_j + J_2 \sum_{\langle\langle ij \rangle\rangle} S_i \cdot S_j + J_3 \sum_{\langle\langle\langle ij \rangle\rangle\rangle} S_i \cdot S_j \,. \quad (1)$$

In Eq. (1), i and j denote Ni sites with spins S_i and S_j, respectively. The parameters J_1, J_2, and J_3 represent the NN, second-NN, and third-NN Heisenberg interactions, respectively. These interactions can be either FM ($J < 0$) or AFM ($J > 0$). For simplicity, the magnitude of spin S is absorbed into Heisenberg interaction parameters, so S is regarded as a unit scalar henceforth. As shown in Fig. S2 of the SM, the FM J_1 and AFM J_3 are dominant in $A_3Ni_2XO_6$, while J_2 is negligible due to its tiny magnitude. Referring to the classical phase diagram for NN FM interactions on honeycomb lattices,[49] the zigzag AFM magnetic ground state of $A_3Ni_2XO_6$ is readily obtained (Fig. S1 in SM).

Although the magnetic ground states of $A_3Ni_2XO_6$ obtained from DFT calculations without SOC are consistent with experimental observations,[34,52] the effects of SOC on the magnetic properties of these Kitaev candidates are generally significant. To clarify this issue, we perform a series of DFT calculations by considering SOC. Similar to the calculations without SOC, the four most likely magnetic orders [Figs. 1(c)–1(f)] are considered to find out the magnetic ground states of $A_3Ni_2XO_6$. For each magnetic order, we consider four representative directions for the alignment of magnetic moments, namely a, b, c, and c^* (i.e., perpendicular to the ab plane). Figure S3 in SM depicts the energy differences of the considered magnetic structures relative to the magnetic ground states. It is evident that the zigzag AFM order remains the most favorable for $A_3Ni_2XO_6$. However, the magnetic easy axes of $A_3Ni_2XO_6$ are slightly different. The magnetic moments tend to be along the c^* axis for NNBO and NNSO, which is consistent with previous works.[34,36,37] As for LNBO (i.e., $Li_3Ni_2BiO_6$) and LNSO, we find that the lowest energies occur when their magnetic moments align along the c axis. According to a previous observation, the Ni spins of LNSO align alongthe c^* axis at very low temperatures.[52] Based on our additional calculations, we find that this difference is mainly due to subtle differences in lattice constants of LNSO (Table S2 in SM). In addition, the incompletely quenched orbital moments suggest that their orbital angular momentum components are active (Table S3 in SM). In other words, the sizable orbital moment, which can give rise to Kitaev interactions, may be achieved through external regulation in $A_3Ni_2XO_6$. In summary, the magnetic ground states of $A_3Ni_2XO_6$ can be characterized as nearly out-of-plane zigzag AFM orders.

It is usually held that a strong SOC plays a crucial role in the emergence of Kitaev interactions, although the Kitaev interaction is also related to Hubbard U, crystal field splitting, and Hund's coupling.[53] Therefore, whether the SOC is sufficiently strong to support the presence of Kitaev interactions in $A_3Ni_2XO_6$ deserves detailed investigations. To comprehensively and accurately study the magnetic interactions of $A_3Ni_2XO_6$ with SOC being considered, we adopt a general bilinear exchange Hamiltonian that incorporates the possible Kitaev interactions as well as off-diagonal terms.[14] It is worth noting that the Dzyaloshinskii–Moriya interaction vanishes due to the inversion symmetry of the $C2/m$ space group. Thus, the spin exchange Hamiltonian under consideration can be simplified to the following form:

$$H = \sum_{ij \in \alpha\beta(\gamma)} \left(J_{ij} \boldsymbol{S}_i \cdot \boldsymbol{S}_j + K_{ij} S_i^\gamma S_j^\gamma + \boldsymbol{S}_i \cdot \boldsymbol{\Gamma}_{ij} \cdot \boldsymbol{S}_j \right) . \quad (2)$$

In Eq. (2), i and j denote Ni sites, and $\boldsymbol{S}_i$ represents the spin operator with components S_i^{α} ($\alpha = x, y, z$). Here, x, y, and z represent the three orthogonal Ni-O bond directions, as shown by the yellow dashed linesin Fig. 1(a). The terms J_{ij}, K_{ij} and $\boldsymbol{\Gamma}_{ij}$ correspond to the Heisenberg interaction, bond-dependent Kitaev interaction, and symmetric off-diagonal exchange parameters, respectively. Note that the $\boldsymbol{\Gamma}_{ij}$ term generally takes the following form:[10]

$$\begin{aligned}\boldsymbol{S}_i \cdot \boldsymbol{\Gamma}_{ij} \cdot \boldsymbol{S}_j \;=\; & \Gamma_{ij}^{x}\left(S_i^{y}S_j^{z} + S_i^{z}S_j^{y}\right) + \Gamma_{ij}^{y}\left(S_i^{z}S_j^{x} + S_i^{x}S_j^{z}\right) \\ & + \Gamma_{ij}^{z}\left(S_i^{x}S_j^{y} + S_i^{y}S_j^{x}\right) . \end{aligned} \tag{3}$$

Similar to the case without SOC, we consider only the first three NN magnetic interactions. Additionally, the magnitude of spin $\boldsymbol{S}$ is also absorbed into the magnetic interaction parameters so that $\boldsymbol{S}$ is treated as a unit vector.

Figure 2 illustrates the calculated magnetic interaction parameters for $A_3Ni_2XO_6$. As shown in Fig. 2(a), all $A_3Ni_2XO_6$ exhibit NN FM and long-range third-NN AFM Heisenberg interactions, which are consistent with the aforementioned results without SOC. Compared to the Heisenberg interactions, the NN, second-NN, and third-NN Kitaev interactions are exceedingly small. This observation appears to deviate from previous theoretical predictions,[26] as the Kitaev interactions are not even significant terms. As shown in Fig. 2(c), we find that the three components of the symmetric off-diagonal exchange Γ are also minimal, with some being FM and others AFM. Clearly, the NN FM and third-NN AFM Heisenberg interactions remain dominant, even when the SOC is taken into account. Consequently, the zigzag AFM magnetic ground state (Fig. S3 of the SM) can stably exist in $A_3Ni_2XO_6$.

To further validate the results obtained from the four-state method, we performed parallel tempering Monte Carlo (PTMC) simulations based on Eq. (2). The resulting magnetic ground states exhibit the experimentally observed zigzag AFM order. The magnetic transition temperatures (i.e., Néel temperature T_N) are estimated to be 10.6 K (NNBO), 12.7 K (NNSO), 12.7 K (LNBO), and 12 K (LNSO), respectively. These values of T_N are close to experimental measurements except for LNBO, whose T_N is higher than the experimental value (5.5 K).[34,36,45] This indicates that the general bilinear exchange Hamiltonian may be incomplete, hinting at the necessity of including higher-order exchange coupling interactions. For instance, the biquadratic exchange interactions may play a significant role in 2D magnets with edge-shared octahedra, such as $NiCl_2$ monolayers.[54] Therefore, we employ a modified Hamiltonian that incorporates the biquadratic (B) term and eliminates relatively minor parameters,

$$H = \sum_{\langle ij \rangle}\left[J_1 \boldsymbol{S}_i \cdot \boldsymbol{S}_j + B\left(\boldsymbol{S}_i \cdot \boldsymbol{S}_j\right)^2\right] + \sum_{\langle\langle\langle ij \rangle\rangle\rangle} J_3 \boldsymbol{S}_i \cdot \boldsymbol{S}_j \,. \tag{4}$$

Here we focus on the major NN Heisenberg interaction, the third-NN Heisenberg interaction, and the newly introduced biquadratic interaction. We use the small angle method to estimate the potential biquadratic exchange

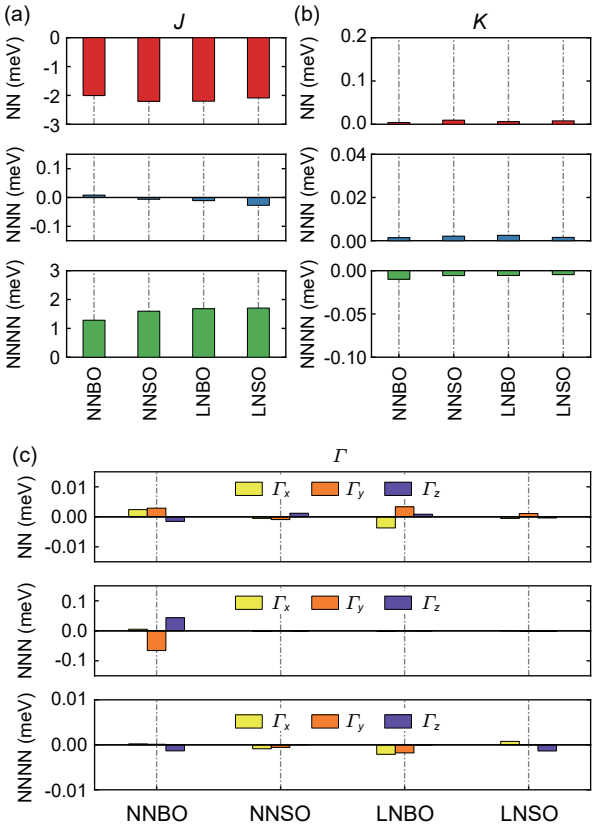

Fig. 2. DFT+SOC calculated magnetic interaction parameters of the general bilinear spin exchange Hamiltonian, Eq. (2). (a) Heisenberg interaction J. (b) Kitaev interaction K. (c) Symmetric off-diagonal exchange Γ.

interaction.[38] Interestingly, sizable biquadratic interactions are indeed obtained for $A_3Ni_2XO_6$ [Fig. S4(c) of the SM]. The biquadratic interaction values of NNBO, NNSO, LNBO, and LNSO are approximately -0.48, -0.22, -0.55, and -0.38 meV, respectively. It is worth noting that the value of NNBO obtained here agrees well with another theoretical study.[55]

Subsequently, PTMC simulations based on Eq. (4) yield T_N of approximately 12 K (NNBO), 12 K (NNSO), 13.4 K (LNBO), and 12.7 K (LNSO), respectively. While the inclusion of biquadratic interactions has an impact on T_N, the resulting changes are relatively minor. Also, the T_N of LNBO is higher than the experimental one.[45] To the best of our knowledge, no research has yet reported the reason why it differs obviously from the other three compounds, which may warrant further study in the future. In fact, biquadratic interactions have been reported to contribute to a systematic rise in the Néel temperature from $FePS_3$ to $NiPS_3$.[56] Moreover, we obtain zigzag ground states based on Eq. (4) likewise. Although the presence of biquadratic interaction does not alter the magnetic ground states of $A_3Ni_2XO_6$, it may induce other effects such as unconventional phase transitions and specific magnetic ordering patterns. For example, biquadratic interaction plays a crucial role in stabilizing ferromagnetism in $NiCl_2$ monolayers.[54] In $CrMnI_6$, a honeycomb magnet, biquadratic interaction favors a Berezinskii–Kosterlitz–Thouless-like transition as the system reduces

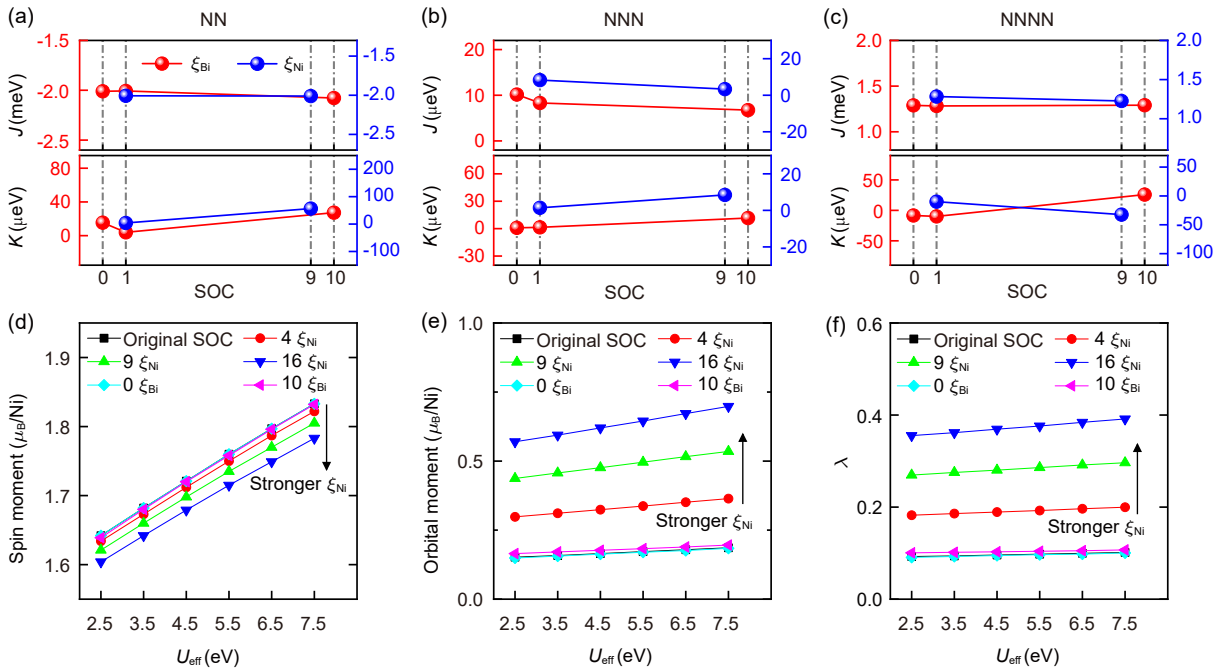

Fig. 3. (a)–(c) Variation of Heisenberg interaction J and Kitaev interaction K with varying SOC strength ξ in NNBO. (a), (b) and (c) show the NN, second-NN and third-NN interactions, respectively. (d)–(f) The spin moment, orbital moment (in units of μ_B/Ni), and λ with different SOC and effective electron correlation U_{eff} in NNBO. Here, 0 ξ_{Bi} and 10 ξ_{Bi} indicate that the SOC of Bi is turned off and enhanced to 0 and 10 times its original value, respectively. The same goes for other expressions.

its temperature from the paramagnetic phase.[57] Specifically, it has been demonstrated that the 1/3 magnetization plateau arises from the interplay between biquadratic interaction and single-ion anisotropy.[55] Additionally, there are some field effects attributed to biquadratic interaction in NNBO such as full or partial spin flop.[55] Furthermore, the biquadratic interaction can induce a novel unconventional ferro-quadrupolar ordered spin nematic phase in spin-1 honeycomb lattice.[58] Therefore, it is essential to include biquadratic interactions when modeling the magnetism of $A_3Ni_2XO_6$ to accurately describe its magnetic properties.

To investigate the effect of SOC on magnetic interactions, we take NNBO as an example and artificially vary its SOC strength. As shown in Figs. 3(a)–3(c), the SOC strength of Bi atoms is first enhanced to 10 times its original value. It is found that all Heisenberg and Kitaev interactions exhibit minimal variation, and the NN FM and long-range third-NN AFM Heisenberg interaction are still dominant. Notably, the Kitaev interactions remain on the order of μeV in magnitude, despite a slight enhancement. In other words, the desired strong SOC for magnetic ions Ni^{2+} does not emerge through proximity to the heavy Bi atoms, and the Kitaev interactions are not significantly enhanced as predicted[26] even when the SOC is enhanced. When the SOC of Bi atoms is turned off, the magnetic interactions similarly exhibit minimal variation. Therefore, it is suggested that the strong SOC of Bi atoms does not significantly influence the Kitaev interactions in NNBO.

Another crucial question is how magnetic interactions are affected by directly varying the SOC of Ni atoms. Given that Kitaev interactions strongly depend on spin–orbit entanglement, we exclusively enhance the SOC of Ni atoms instead of reducing it. According to previous reports on well-known Kitaev candidates, the SOC constants of Ir in Na_2IrO_3 and Ru in $RuCl_3$ are 0.4 eV and 0.13 eV,[9,11] respectively. The SOC constant of free Ni^{2+} is approximately 0.0425 eV.[59] To make the SOC strength of Ni^{2+} comparable to those of Na_2IrO_3 and $RuCl_3$, we need to increase it to 9 times the original value. Figures 3(a)–3(c) illustrate the results when the SOC strength of Ni atoms is directly enhanced to 9 times its original value. Similar to the aforementioned situation where the SOC of Bi atoms is enhanced, the dominant Heisenberg interactions exhibit minimal change, while the Kitaev interactions are still very weak (on the order of μeV). Moreover, it is observed that the enhanced SOC, whether in Bi atoms or Ni atoms, does not significantly affect the strength of symmetric off-diagonal interactions $\boldsymbol{\Gamma}$ (see Fig. S5 of the SM). In other words, symmetric off-diagonal interactions $\boldsymbol{\Gamma}$ remain significantly weaker compared with Heisenberg interactions J. Overall, enhancing the SOC of either Bi or Ni atoms neither strengthens the Kitaev interactions nor alters the dominant nature of Heisenberg interactions.

The Kitaev interaction is highly dependent on the hopping integrals of its specific bonds,[26] where the strength is determined by the overlap of relevant orbitals. Obviously, a substantial orbital moment is critical for generating Kitaev interactions. In light of this, we systematically examine both spin and orbital magnetic moments under varying SOC and effective electron correlation U_{eff} in NNBO. As shown in Figs. 3(d) and 3(e), the SOC of Bi atoms

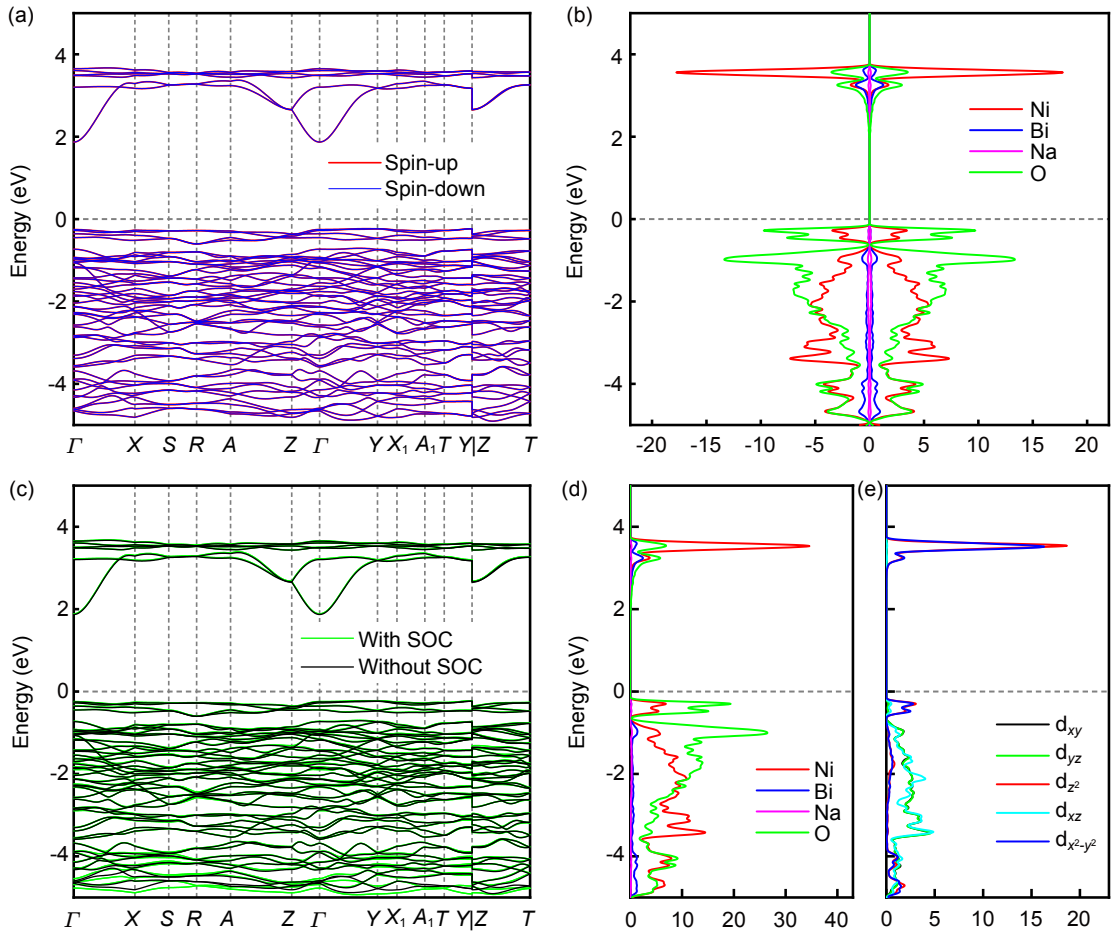

Fig. 4. Electronic structures of NNBO. (a) Band structure without SOC. (b) The PDOS without SOC. (c) Comparisons between the band structures with SOC and without SOC. (d) PDOS with SOC. (e) PDOS of 3d orbitals of Ni atoms.

has a negligible effect on either spin or orbital magnetic moments. This finding supports the conclusion that the strong SOC of Bi atoms does not contribute to the generation of Kitaev interactions. In addition, it is observed that the spin magnetic moment decreases slightly, while the orbital magnetic moment increases significantly with the enhancement of the SOC of Ni atoms. This indicates that the orbital degree of freedom will become increasingly active as the SOC of Ni atoms is enhanced. To clearly quantify the significance of the orbital degree of freedom, we define a dimensionless parameter λ as the ratio of the orbital magnetic moment to spin magnetic moment. As illustrated in Fig. 3(f), λ increases with the enhancement of SOC for Ni atoms. However, the orbital magnetic moment is never dominant compared to $J_{\rm eff} = 1/2$ state in well-known Kitaev QSL candidates.[6,15] Specifically, the orbital magnetic moment is approximately twice the spin magnetic moment in well-known Kitaev magnet Na_2IrO_3.[60] In addition, it is evident that $U_{\rm eff}$ has minimal effect on both the orbital magnetic moment and λ. In summary, a significant orbital moment which is essential for Kitaev interactions cannot be achieved by tuning either SOC or $U_{\rm eff}$ in NNBO.

To gain a deeper insight into how the SOC affects magnetic interactions, we further investigate the electronic structures of $A_3Ni_2XO_6$ by neglecting and including the SOC, respectively. As a representative example, we first examine NNBO and present its electronic structures without SOC in Figs. 4(a) and 4(b). The spin-up and spin-down channels show degeneracy in the band structure. Furthermore, the projected density of states (PDOS) of NNBO reveals that its electronic states near the Fermi level primarily originate from Ni and O atoms, and that its spin-up and spin-down DOSs are identical due to the AFM order. As depicted in Fig. 4(c), we also illustrate the difference in the band structure with and without SOC. It is noted that SOC has minimal effect on the band structure. In particular, the bands near the Fermi level exhibit negligible changes. As shown in Fig. 4(d), the PDOSs indicate that states near the Fermi level are still primarily contributed by Ni and O atoms, similar to the case without SOC.

Given the weak SOC of the O atom and the fact that the magnetism of NNBO is primarily contributed by the 3d orbitals of the Ni atom, we present their PDOSs in Fig. 4(e). The conduction band states above the Fermi level are primarily contributed by d_{z^2} and $d_{x^2-y^2}$ orbitals, whereas the lower valence band states originate from d_{xy}, d_{yz}, and d_{xz} orbitals. This indicates that the magnetic ions Ni^{2+} exhibit a $3d^8$ electronic configuration with half-filled e_g orbitals and fully filled t_{2g} orbitals. Consequently,

the orbital moment originates from the two e_g orbitals rather than from three fully filled t_{2g} orbitals. It is accepted that direct exchange between two half-filled orbitals generally yields an AFM interaction due to Pauli exclusion principle. Nevertheless, the NN Heisenberg interaction of NNBO is found to be FM [Fig. 2(a)]. Thus, NN FM Heisenberg interactions cannot be solely attributed to direct exchange mechanisms. Similar to the case of $3d^7$ Kitaev candidates,[15,16] superexchange mediated by neighboring O^{2-} anions plays a pivotal role in determining magnetic interactions. Moreover, the electronic structures of NNSO, LNBO, and LNSO exhibit similar characteristics (Figs. S6–S8 in SM). These results suggest that superexchange processes play a significant role in generating magnetic interactions, especially NN FM Heisenberg interactions of $A_3Ni_2XO_6$.

Next, we further explore the effect of the superexchange process on magnetic interactions. The NN superexchange process between magnetic ions Ni^{2+} is mediated by the 2p orbitals of intermediate O^{2-} anions. As shown in Fig. 1(a), the bond angle of the superexchange pathway Ni-O-Ni is approximately 90°. According to the well-established Goodenough–Kanamori rule,[61,62] two magnetic ions Ni^{2+} with a 90° bond angle and half-filled e_g orbitals generally exhibit FM superexchange interaction. In addition, the 3d orbital of the transition metal is highly localized, leading to significant Coulomb interactions and relatively small direct hopping parameters. As a result, the dominant superexchange mechanism gives rise to the NN FM Heisenberg interaction, as predicted by our DFT calculations [Fig. 2(a)]. On the other hand, the superexchange process does not appear to generate significant Kitaev interactions [Fig. 2(b)], which is inconsistent with previous theoretical predictions.[26] In previous studies[15,16] on the high-spin state of $3d^7$ (i.e., $t_{2g}^5e_g^2$ electronic configuration), it was proposed that the Kitaev interactions originate from hopping processes between t_{2g} orbitals and those between t_{2g} and e_g orbitals. However, Ni^{2+} has a $3d^8$ (i.e., $t_{2g}^6e_g^2$) electronic configuration and hopping processes between t_{2g} electrons are forbidden, which may explain the weakness of Kitaev interactions. In fact, Kitaev interaction is only significant (approximately twice that of Heisenberg interaction) if Hund's coupling of p orbitals of anions is close to zero.[26] In realistic magnetic materials such as $A_3Ni_2XO_6$, Hund's coupling is typically non-negligible. Accordingly, it is reasonable that Kitaev interactions are extremely weak in $A_3Ni_2XO_6$.

We also investigate the electronic structures under varying strengths of SOC in Bi and Ni atoms. NNBO is again chosen as a representative example. As depicted in Figs. S9 and S10 in SM, a stronger SOC of Bi atoms primarily leads to more pronounced band splitting and cannot disrupt the $t_{2g}^6e_g^2$ electronic configuration. Additionally, it is observed that the states of Ni atoms are closer to the Fermi level and that the states of Bi near the Fermi level remain sparse. Moreover, hybridization between Ni and Bi atoms is negligible. As a result, both the orbital magnetic moment and λ exhibit negligible change [Figs. 3(e) and 3(f)]. Even with enhanced SOC in Bi atoms, the Kitaev interactions are not induced by enhancing the SOC in Ni atoms through the proximity effect [Figs. 3(a)–3(c)]. Further, the electronic structures of NNBO with an enhanced SOC in Ni atoms are presented in Fig. S11 in SM. The results differ slightly from the case in which the SOC of Bi atoms is enhanced. Although both the orbital magnetic moment and λ increase with the enhancement of the SOC of Ni atoms, a dominant orbital moment remains absent. As for NNSO, LNBO, and LNSO, enhancing the SOC strength of either Bi or Ni atoms similarly fails to induce a dominant orbital moment (Figs. S12–S14 in SM). Hence, the enhanced SOC of Ni atoms is insufficient to generate the necessary spin–orbit entangled states for bond-dependent Kitaev interactions despite the SOC mixing different orbital and spin moments.

Finally, we explore the impact of strain on the magnetic properties of NNBO. Here, we consider applying a 5% strain to NNBO. First, we examine the magnetic ground state of the strained NNBO with SOC taken into account. As shown in Fig. S15 in SM, the strained NNBO still favors the zigzag AFM order. Next, we calculate magnetic interaction parameters defined in Eq. (2). As illustrated in Fig. S16 in SM, the Kitaev interaction and symmetric off-diagonal exchange Γ remain small. Meanwhile, the NN FM and long-range third-NN AFM Heisenberg interactions remain dominant [Fig. S16(a) in SM]. These dominant Heisenberg interactions also stabilize the zigzag AFM ground state (Fig. S15 in SM). Furthermore, we analyze the electronic structures of the strained NNBO. Similar to the unstrained case (Fig. 4), the SOC has little effect on band structure, and the $3d^8$ electronic configuration with half-filled e_g orbitals persists (Fig. S17 in SM). As shown in Table S4 in SM, the orbital magnetic moment ($0.134\,\mu_B$/Ni) is even smaller than its original value ($0.165\,\mu_B$/Ni). Although atoms are brought closer together in strained NNBO—potentially increasing hopping parameters—the fundamental physics governing Kitaev interactions remains unchanged. Similarly, we examine the orbital magnetic moment of strained NNBO under varying U_{eff} and SOC in Fig. S18 of the SM. The orbital moment remains insignificant compared to spin moment. Overall, strain does not induce Kitaev interactions, and strained NNBO retains its zigzag AFM order without significant Kitaev contributions.

4. Conclusions. In summary, we investigate the magnetic properties, with a particular focus on Kitaev interactions, in $S = 1$ honeycomb magnets $A_3Ni_2XO_6$ using first-principles calculations and Monte Carlo simulations. We find that $A_3Ni_2XO_6$ are the antiferromagnets with zigzag order, consistent with previous studies. Moreover, most of their zigzag magnetic orders favor out-of-plane magnetic moments. The dominant magnetic interactions are the NN FM Heisenberg, long-range third-NN AFM Heisenberg and biquadratic interactions. Furthermore, the potential Kitaev interactions are extremely weak in $A_3Ni_2XO_6$. We demonstrate that neither the enhanced SOC of Ni nor that of Bi atoms induces Kitaev interactions or significantly affects the strength of the dominant Heisenberg interactions. By analyzing the electronic structures and the mechanisms

underlying magnetic interactions, we suggest that neither tuning the SOC strength nor applying a strain can generate sufficient spin–orbit entangled states to realize bond-dependent Kitaev interactions. Our work not only helps to deepen understanding of the intriguing magnetic properties of $A_3Ni_2XO_6$ but also provides insights for exploring Kitaev physics in these materials.

Acknowledgements. This work was supported by the National Key R&D Program of China (Grant Nos. 2024YFA1408303 and 2022YFA1403301), the National Natural Sciences Foundation of China (Grant Nos. 12474247 and 92165204). Yusheng Hou acknowledges the support from Guangdong Provincial Key Laboratory of Magnetoelectric Physics and Devices (Grant No. 2022B1212010008) and Research Center for Magnetoelectric Physicsof Guangdong Province (Grant No. 2024B0303390001). DFT calculations are performed on Tianhe-Xingyi.

References

[1] Balents L 2010 *Nature* **464** 199
[2] Broholm C, Cava R J, Kivelson S A, Nocera D G, Norman M R, and Senthil T 2020 *Science* **367** eaay0668
[3] Kitaev A 2006 *Ann. Phys.* **321** 2
[4] Savary L and Balents L 2017 *Rep. Prog. Phys.* **80** 016502
[5] Hermanns M, Kimchi I, and Knolle J 2018 *Annu. Rev. Condens. Matter Phys.* **9** 17
[6] Jackeli G and Khaliullin G 2009 *Phys. Rev. Lett.* **102** 017205
[7] Chaloupka J, Jackeli G, and Khaliullin G 2010 *Phys. Rev. Lett.* **105** 027204
[8] Plumb K W, Clancy J P, Sandilands L J, Shankar V V, Hu Y F, Burch K S, Kee H Y, and Kim Y J 2014 *Phys. Rev. B* **90** 041112
[9] Chaloupka J, Jackeli G, and Khaliullin G 2013 *Phys. Rev. Lett.* **110** 097204
[10] Rau J G, Lee E K, and Kee H Y 2014 *Phys. Rev. Lett.* **112** 077204
[11] Banerjee A, Bridges C A, Yan J Q *et al.* 2016 *Nat. Mater.* **15** 733
[12] Winter S M, Li Y, Jeschke H O, and Valentí R 2016 *Phys. Rev. B* **93** 214431
[13] Hou Y S, Xiang H J, and Gong X G 2017 *Phys. Rev. B* **96** 054410
[14] Hou Y S, Yang J H, Xiang H J, and Gong X G 2018 *Phys. Rev. B* **98** 094401
[15] Liu H and Khaliullin G 2018 *Phys. Rev. B* **97** 014407
[16] Sano R, Kato Y, and Motome Y 2018 *Phys. Rev. B* **97** 014408
[17] Liu H, Chaloupka J, and Khaliullin G 2020 *Phys. Rev. Lett.* **125** 047201
[18] Motome Y, Sano R, Jang S, Sugita Y, and Kato Y 2020 *J. Phys.: Condens. Matter* **32** 404001
[19] Songvilay M, Robert J, Petit S *et al.* 2020 *Phys. Rev. B* **102** 224429
[20] Kim C, Jeong J, Lin G *et al.* 2021 *J. Phys.: Condens. Matter* **34** 045802
[21] Lin G, Jeong J, Kim C *et al.* 2021 *Nat. Commun.* **12** 5559
[22] Samarakoon A M, Chen Q, Zhou H, and Garlea V O 2021 *Phys. Rev. B* **104** 184415
[23] Sanders A L, Mole R A, Liu J, Brown A J, Yu D, Ling C D, and Rachel S 2022 *Phys. Rev. B* **106** 014413
[24] Yan J Q, Okamoto S, Wu Y, Zheng Q, Zhou H D, Cao H B, and McGuire M A 2019 *Phys. Rev. Mater.* **3** 074405
[25] Gu Y, Li X, Chen Y *et al.* 2024 *Phys. Rev. B* **109** L060410
[26] Stavropoulos P P, Pereira D, and Kee H Y 2019 *Phys. Rev. Lett.* **123** 037203
[27] Xu C, Feng J, Kawamura M, Yamaji Y, Nahas Y, Prokhorenko S, Qi Y, Xiang H, and Bellaiche L 2020 *Phys. Rev. Lett.* **124** 087205
[28] Xu C, Feng J, Xiang H, and Bellaiche L 2018 *npj Comput. Mater.* **4** 57
[29] Lee I, Utermohlen F G, Weber D, Hwang K, Zhang C, van Tol J, Goldberger J E, Trivedi N, and Hammel P C 2020 *Phys. Rev. Lett.* **124** 017201
[30] Cen J and Kee H Y 2023 *Phys. Rev. B* **107** 014411
[31] Amoroso D, Barone P, and Picozzi S 2020 *Nat. Commun.* **11** 5784
[32] Li X Y, Xu C S, Liu B Y, Li X Y, Bellaiche L, and Xiang H J 2023 *Phys. Rev. Lett.* **131** 036701
[33] Huang C, Liu B, Jiang L, Pan Y, Fan J, Shi D, Ma C, Luo Q, and Zhu Y 2023 *Phys. Rev. B* **108** 094433
[34] Zvereva E A, Stratan M I, Ovchenkov Y A *et al.* 2015 *Phys. Rev. B* **92** 144401
[35] Shangguan Y, Bao S, Dong Z Y *et al.* 2023 *Nat. Phys.* **19** 1883
[36] Seibel E M, Roudebush J H, Wu H, Huang Q, Ali M N, Ji H, and Cava R J 2013 *Inorg. Chem.* **52** 13605
[37] Shi X, Cui Y, Shangguan Y *et al.* 2024 *Chin. Phys. B* **33** 067601
[38] Zhu H F, Cao H Y, Xie Y, Hou Y S, Chen S Y, Xiang H J, and Gong X G 2016 *Phys. Rev. B* **93** 024511
[39] Kresse G and Hafner J 1993 *Phys. Rev. B* **47** 558
[40] Kresse G and Furthmüller J 1996 *Phys. Rev. B* **54** 11169
[41] Kresse G and Furthmüller J 1996 *Comput. Mater. Sci* **6** 15
[42] Perdew J P, Burke K, and Ernzerhof M 1996 *Phys. Rev. Lett.* **77** 3865
[43] Blochl P E 1994 *Phys. Rev. B* **50** 17953
[44] Dudarev S L, Botton G A, Savrasov S Y, Humphreys C J, and Sutton A P 1998 *Phys. Rev. B* **57** 1505
[45] Berthelot R, Schmidt W, Muir S, Eilertsen J, Etienne L, Sleight A W, and Subramanian M A 2012 *Inorg. Chem.* **51** 5377
[46] Zvereva E A, Evstigneeva M A, Nalbandyan V B, Savelieva O A, Ibragimov S A, Volkova O S, Medvedeva L I, Vasiliev A N, Klingeler R, and Buechner B 2012 *Dalton Trans.* **41** 572
[47] Yuan D, Liang X, Wu L, Cao Y, Ai X, Feng J, and Yang H 2014 *Adv. Mater.* **26** 6301
[48] Xiang H J, Kan E J, Wei S H, Whangbo M H, and Gong X G 2011 *Phys. Rev. B* **84** 224429
[49] Fouet J B, Sindzingre P, and Lhuillier C 2001 *Eur. Phys. J. B* **20** 241
[50] Li P H Y, Bishop R F, Farnell D J J, and Campbell C E 2012 *Phys. Rev. B* **86** 144404
[51] Zhou Y M, Geng W T, and Wang D S 1998 *Phys. Rev. B* **57** 5029
[52] Kurbakov A I, Korshunov A N, Podchezertsev S Y *et al.* 2017 *Phys. Rev. B* **96** 024417
[53] Winter S M, Tsirlin A A, Daghofer M, van den Brink J, Singh Y, Gegenwart P, and Valenti R 2017 *J. Phys.: Condens. Matter* **29** 493002
[54] Ni J Y, Li X Y, Amoroso D, He X, Feng J S, Kan E J, Picozzi S, and Xiang H J 2021 *Phys. Rev. Lett.* **127** 247204
[55] Chen Z F, Zhang B H, Zhu W Q, Li L C, Liu B Y, Feng J S, Xu C S, and Xiang H J 2024 arXiv:2406.03338v2 [cond-mat.str-el]
[56] Amirabbasi M and Kratzer P 2024 *Phys. Rev. Mater.* **8** 084005
[57] Zhang S, Li X, Zhang H, Cui P, Xu X, and Zhang Z 2023 *npj Quantum Mater.* **8** 38
[58] Mashiko T and Okubo T 2024 *Phys. Rev. Res.* **6** 033110
[59] Blume M and Watson R E 1963 *Proc. R. Soc. Lond. A* **271** 565
[60] Kim B J, Jin H, Moon S J *et al.* 2008 *Phys. Rev. Lett.* **101** 076402
[61] Goodenough J B 1958 *J. Phys. Chem. Solids* **6** 287
[62] Kanamori J 1959 *J. Phys. Chem. Solids* **10** 87